Prediction of a Non-Valence Temporary Anion State of $(NaCl)_2$

Journal:	*The Journal of Physical Chemistry*
Manuscript ID	jp-2019-07782w.R1
Manuscript Type:	Special Issue Article
Date Submitted by the Author:	n/a
Complete List of Authors:	Kairalapova, Arailym; University of Pittsburgh, Chemistry Jordan, Kenneth; University of Pittsburgh, Department of Chemistry; Falcetta, Michael; Grove City College, Department of Chemistry Steiner, Dalton; Grove City College Sutter, Brittni; Grove City College Gowen, Josiah; Grove City College

Prediction of a Non-valence Temporary Anion State of $(NaCl)_2$

Arailym Kairalapova, and Kenneth D. Jordan*

Department of Chemistry, University of Pittsburgh, Pittsburgh, PA 15260

Michael F. Falcetta, Dalton K. Steiner, Brittni L. Sutter, Josiah S. Gowen

Department of Chemistry, Grove City College, Grove City, PA 16127

*Jordan@pitt.edu

ABSTRACT: The equation-of-motion coupled cluster method is used to characterize the low-lying anion states of $(NaCl)_2$ in its rhombic structure. This species is known to possess a non-valence bound anion of A_g symmetry. Our calculations also demonstrate that it has a non-valence temporary anion of B_{2u} symmetry, about 14 meV above threshold. The potential energy curves of the two anion states and of the ground state of the neutral molecule are reported as a function of distortion along the symmetric stretch normal coordinate. Implications for experimental detection of the temporary anion state are discussed. The sensitivity of the results to the inclusion of high-order correlation effects and of core correlation is examined.

I. INTRODUCTION

Anionic states of molecules and clusters play important roles in many chemical processes. Anions can be characterized as valence or non-valence, depending on the nature of the electron-molecule interaction potential, with short-range interactions proving most important for valence anions and long-range electrostatics and/or correlation effects being responsible for the existence of non-valence anions. Anions can also be classified as bound or unbound, depending on their energy relative to that of the ground state neutral system, with bound anions being energetically more stable than the electronic ground state of the neutral system and unbound anions being less stable, and hence subject to electron autodetachment. The relative energy of the anion and neutral may also change upon distortion of the molecular geometry, and care must be taken to clearly indicate the geometry under consideration. In some non-valence bound anions, the electrostatic attraction alone is sufficient to bind the electron, which means that the electron is bound in the Koopmans' Theorem (KT) approximation[1] when employing sufficiently flexible basis sets. (Here we are assuming that electron correlation effects do not lead to a significant change in the electrostatic potential.) The best known non-valence bound anions are dipole-bound anions.[2–4] There are also reports of non-valence quadrupole-bound anions[5,6] although we note that some anions that have been reported as quadrupole-bound actually fail to bind the excess electron in the KT and Hartree-Fock (HF) approximations, indicating that correlation effects are necessary for binding. We classify anions in which correlation and relaxation effects in response to correlation play a determinative role in the binding as non-valence correlation-bound (NVCB),[7–10] even though electrostatics may also play an important role in the binding.

While bound anions are most familiar to chemists, unbound anions, also referred to as temporary anions (TAs), can play a vital role in a range of processes including vibrational and electronic excitation and chemical bond cleavage.[11–13] In addition to the valence vs non-valence classification, TAs can be further classified in terms of the mechanism giving rise to the trapping of the excess electron. In this study

we are interested in non-valence TAs for which the trapping is primarily due to an angular momentum barrier. Such anions are also referred to as shape resonances.[11]

Recently we introduced a model $(H_2O)_4$ cluster for analyzing the relative importance of electrostatics and correlation effects in the binding of an excess electron in a non-valence anion.[10] The water molecules in the cluster were arranged so as to give D_{2h} symmetry, and, thus, to have no net dipole. By decreasing the separation between the two dimer subunits, the A_g ground-state anion changes from bound to unbound at the KT level, although when electron correlation effects are included by means of the electron affinity equation-of-motion coupled cluster singles plus doubles (EA-EOM-CCSD) method,[14] the anion is found to be bound for the entire range of geometries considered. In a subsequent paper we showed that for a range of geometries the $(H_2O)_4$ model also possesses a non-valence temporary anion state.[15] Though there are reports of non-valence TAs of molecules with sizable dipole moments, non-polar systems are of interest because their long-range electrostatic attraction falls off more rapidly than r^{-2} (where r is the electron-molecule distance), and hence, when combined with a non-zero angular momentum contribution gives rise to a barrier for trapping an excess electron.[16,17]

While the arrangement of water monomers in the $(H_2O)_4$ model considered in References 10 and 15 is unrealizable experimentally, the model provides valuable insights into the characteristics required of an experimentally realizable, nonpolar molecule or cluster likely to possess a low-energy non-valence temporary anion. Specifically, the system should possess a NVCB anion state belonging to the totally symmetric representation of the relevant point group. The natural orbital or Dyson orbital[18] associated with the excess electron in such anion states is largely *s*-like at distances outside the molecular region. This suggests the possibility of excited *p*-like non-valence anion states, which, depending on the strength of the attraction, would be weakly bound or unbound. The *p*-like character is important as this leads to an angular momentum barrier that can contribute to the trapping of the excess electron. This consideration suggests that the rhombic $(NaCl)_2$ cluster is an ideal candidate for a non-valence temporary anion, as it has been predicted to have a bound non-valence anion state of A_g symmetry.[19,20] In the study of

Anusiewicz et al.[19] $(NaCl)_2$ was reported to have a vertical electron binding energy (EBE) of 23 and 144 meV at the KT and coupled cluster singles and doubles with perturbative triples [CCSD(T)][21] levels of theory, respectively. (In the sign convention used in the present study, a positive EBE refers to a abound anion.) Similar results were reported by Sommerfeld et al.[20] who reported KT and EA-EOM-CCSD values of the EBE.

The lowest unoccupied molecular orbital (LUMO) from a HF calculation on the neutral $(NaCl)_2$ cluster is shown in Figure 1 from which it is seen that the LUMO is well described as the bonding combination of *sp* hybridized orbitals associated with each Na atom, with the charge being localized outside the ring to minimize repulsion with the Cl^- ions. (The basis set and cluster geometry used for these calculations is described in Section II.) Since the A_g anion is only weakly bound, one might anticipate that the B_{2u} anion state resulting from the anti-bonding combination of the hybridized orbitals associated with the two Na atoms, would lie energetically above the neutral cluster. In this study we use EOM methods to characterize the B_{2u} anion state of rhombic $(NaCl)_2$ to determine if it is indeed temporary in nature at the equilibrium geometry of the neutral cluster. We note that the existence of excited state non-valence anions, whether bound or unbound, is relevant for understanding the capture of low-energy electrons, and possibly also the formation of nuclear Feshbach resonances.[22]

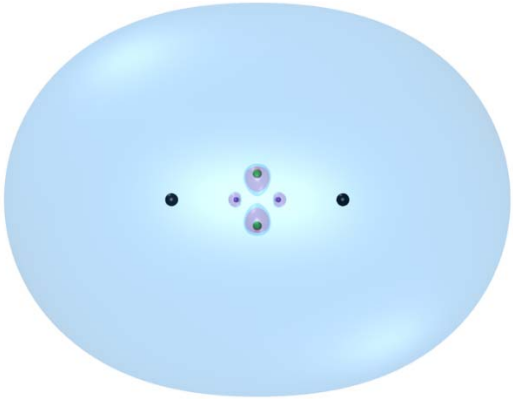

Figure 1. Lowest unoccupied molecular orbital from a Hartree-Fock calculation on neutral $(NaCl)_2$ at q = 0 using the aug-cc-pVTZ basis set on the atoms and two sets of 9*s* functions as described in the text and centered at the location of the two black spheres, on the same axis as the sodium atoms. The contour shown encloses 90% of the charge density.

II. COMPUTATIONAL DETAILS

The geometry of the rhombic form of $(NaCl)_2$ was optimized using the MP2 method[23] in conjunction with the aug-cc-pVTZ basis set and using the frozen core (FC) approximation.[24,25] This geometry was used in a calculation of the harmonic frequencies at the same level of theory. Distortion along the totally symmetric breathing mode (q) was considered in order to follow the B_{2u} anion as it evolves from a bound state to a TA, with a value of $q = 0$ corresponding to the optimized geometry of the neutral cluster. The FC approximation was used in previous studies[19,20] and the geometries considered in the current work are largely based on the geometry and definition of q given above. However, in the course of this work it became apparent that correlating the 2*s* and 2*p* electrons in the sodium atoms had a significant effect on the optimized geometry of the neutral cluster and on the energies of the anion states relative to the neutral. As a result, we also optimized the geometry of the neutral cluster using the MP2 method allowing correlation of the sodium 2*s* and 2*p* electrons using the aug-cc-pCVTZ basis[26] on the Na atoms. (Hereafter calculations including electron correlation and correlating the Na *L*-shell electrons are referred to as correlated core). This geometry of the neutral cluster optimized in the correlated core approximation is close to that obtained by displacing the FC structure to $q = -0.05233$. The normal mode relative displacements calculated in the FC and correlated core approximations are essentially identical.

The main computational approach used in this study to characterize the anion states of $(NaCl)_2$ is the EA-EOM-CCSD method, which has been found to accurately characterize both bound and unbound anion states provided sufficiently flexible basis sets are employed.[8–10, 27–29] In this approach, a CCSD calculation is carried out on the electronic ground state of the neutral molecule, and the resulting T1 and T2 amplitudes are used to carry out a similarity transform of the Hamiltonian which is then used to perform a one-particle (1*p*) plus two particle-one-hole (2*p*1*h*) configuration interaction (CI) calculation on the excess electron state. Calculations are also carried out using the EOM-CCSD(T)(a)* method[30] which accounts in an approximate manner for the contributions of triple excitations to the ground state of the neutral and of 3*p*2*h* excitations in the CI calculation of the anion. The EOM-CCSD(T)(a)* algorithm used

is implemented for excitation energies but can be "tricked" into calculating electron affinities by starting from a closed shell configuration with two excess electrons in a "continuum" orbital.

The orbital depicted in Figure 1 was obtained from a HF calculation on the neutral molecule at q = 0 using the aug-cc-pVTZ basis set supplemented with two sets of diffuse *s* Gaussians located on the Na-Na axis, but with their centers displaced further from the Na atoms from the center of the ring (shown as black spheres in Figure 1). These supplemental sets contained nine even-tempered primitive Gaussians with the largest exponent being 0.25 and each successive exponent being smaller by a factor of $\sqrt{10}$. We note that the LUMO of $(NaCl)_2$ obtained from calculations employing supplemental diffuse *s* and *p* functions on the Na atoms has nearly the same EBE and charge distribution as that obtained with the basis set with the off-atom *s* functions. The use of off-atom basis functions proves beneficial in the procedure used to characterize the B_{2u} anion state at geometries at which it is unbound. The distance of the centers of the supplementary basis functions from the Na atoms was optimized to maximize the binding of the B_{2u} anion state for an expanded ring geometry with q = 0.08 for which the anion state is weakly bound in EA-EOM-CCSD calculations in the correlated core approximation. This resulted in a displacement of 5 Å of the centers of the diffuse sets from the Na atoms. We also checked that it remains close to optimal for q = -0.07 where the B_{2u} anion is temporary with the highest energy considered in this study. This basis set gives a KT value of the vertical EBE (for forming the A_g anion) of 20 meV, 3 meV smaller than that reported by Anusiewicz et al.[19] Moreover, the EA-EOM-CCSD value of the EBE from our calculations (139 meV) employing this basis set and the FC approximation agrees closely with the EA-EOM-CCSD result of Sommerfeld et al.[20]

As noted above, we have also calculated the EBEs as a function of q, the extent of the displacement along the normal coordinate corresponding to the totally symmetric breathing mode of the neutral molecule. As q is varied, the location of the supplemental diffuse *s* functions relative to the sodium atoms was held fixed, displaced 5 Å from the Na atoms. The electronic structure calculations were carried out using CFOUR.[31]

In the Siegert picture[32] temporary anions are characterized by a complex energy

$$E_{res} = E_r - \frac{i\Gamma}{2} \quad (1)$$

where E_r is the resonance position and Γ its width which is proportional to the reciprocal of the lifetime (atomic units have been assumed). Both E_r and Γ are geometry dependent. For geometries at which the B_{2u} anion is unbound, the results from the EA-EOM-CCSD calculations were combined with the stabilization method[33] and analytic continuation[34] to determine the complex energies associated with the temporary anion states. Briefly, the exponents of the supplemental diffuse basis functions were multiplied by a scale factor, β, and the energies of the first seven eigenvalues corresponding to the electron attached states (relative to that of the neutral) are calculated for a series of β values ranging from 0.2 to 1.7.

A plot of the energies of the excess electron states (relative to the energy of the neutral molecule) vs β reveals avoided crossings that can be interpreted as resulting from the mixing of a diabatic discrete state corresponding to the anion (with detachment suppressed) with diabatic discretized representations of the continuum of the free electron plus the neutral molecule. Hereafter, the latter are referred to as DC levels. As is well documented in the literature, the resonance position and width can be extracted using data from the avoided crossing regions.[33–37] In the present study we accomplish this by means of analytic continuation and locating the complex stationary point, β*, for which dE/dβ = 0. In the case of a clear-cut avoided crossing between two levels, the analytic continuation can be carried out by fitting the data in the vicinity of an avoided crossing to the expression

$$P(\beta)E^2 + Q(\beta)E + R(\beta) = 0, \quad (2)$$

where

$$P(\beta) = 1 + p_1\beta + p_2\beta^2 + \cdots \quad (3a)$$

$$Q(\beta) = q_0 + q_1\beta + q_2\beta^2 + \cdots \quad (3b)$$

and

$$R(\beta) = r_0 + r_1\beta + r_2\beta^2 + \cdots \quad (3c)$$

The stationary point β* is substituted back into the expression for the energy to obtain estimates of E_r and Γ. The use of a quadratic rather than a linear expression in E is to accommodate the branch-point structure associated with avoided crossings.[34–36]

For narrow resonances, for which $\Gamma/2 << E_r$, stabilization graphs generally display well-defined avoided crossings between the diabatic discrete state and the discretized continuum (DC) solutions as the scale parameter is varied. However, for resonances for which the value of Γ/2 approaches E_r in magnitude, the avoided crossings become less pronounced. For the geometries of $(NaCl)_2$ considered here semi-quantitative results for the B_{2u} anion can be obtained using the quadratic expression given by eq 2, with the P, Q, and R polynomials being, respectively, of order 3, 4, and 5, in β, and employing data from the two roots involved in an avoided crossing. However, to obtain better converged complex resonance energies, we employed a generalization of eq 2 to include terms of higher order in E. In our application of this approach to extract resonance parameters of the B_{2u} anion of $(NaCl)_2$, we included terms through E^3 for $q = 0.07$ and E^4 for smaller values of q, and using data from three and four roots, respectively. We employ polynomials in eq 2 and its extensions of powers n - m, where m is the power of E in the expression for the energy, and n is an integer ranging from 6 to 13. Typically, more data points were used than parameters in combination with least squares fitting. In addition, for each geometry considered several independent analytic continuation calculations using different sets of data points and different order polynomials in eq 3 were performed, each giving slightly different complex resonance energies, with the average of these results being reported for E_r and Γ.

III. RESULTS AND DISCUSSION

III.1 Stabilization calculations. The stabilization graph obtained from the EA-EOM-CCSD calculations on $(NaCl)_2$ using the correlated core approximation and at $q = 0$ is shown in Figure 2a. The figure also includes the energies of the DC levels obtained by solving for the eigenvalues of the one

electron system using the same basis set as used for the EA-EOM-CCSD calculations but with the nuclear charges set equal to zero. The DC levels were calculated using Gaussian 16.[38] From inspection of the graph it is seen that, for the energy range depicted, the EOM calculations give one more energy level than there are DC levels. This is indicative of the presence TA resonance. It is also seen that the diabatic (i.e., unmixed) discrete state corresponding to the resonance falls near 9 meV. In order to obtain a more accurate value of E_r and to determine the width we use the analytic continuation procedure described above, together with data from the second to fifth roots of the EA-EOM-CCSD calculations for scale factors ranging from 0.2 to 1.0. The resulting average E_r and Γ values are 8.95 and 7.28 meV, respectively.

Figure 2b reproduces the portion of the stabilization graph involving the avoided crossings. In this figure we also indicate the energy of the diabatic discrete state by a horizontal line and color code the eigenvalues involved in the avoided crossings. In addition, we have added lines to indicate the approximate energies of the DC levels when orthogonalized to the discrete level to give so-called orthogonalized DC (ODC) levels. This helps make more transparent that there are two avoided crossings occurring near β values of 0.3 and 0.9. Interestingly, the crossing of the discrete state and the relevant DC levels occur near larger β values (0.40 and 1.33, respectively). The shifts of the avoided crossings to lower β values than those that correspond to the crossings between the discrete level and the DC levels is a consequence of orthogonalization. If we treat the region near an avoided crossing as a two level system, then the eigenvalue problem becomes

$$\begin{pmatrix} H_{11} - E & V - SE \\ V - SE & H_{22} - E \end{pmatrix} \begin{pmatrix} c_1 \\ c_2 \end{pmatrix} = \begin{pmatrix} 0 \\ 0 \end{pmatrix} \quad (4)$$

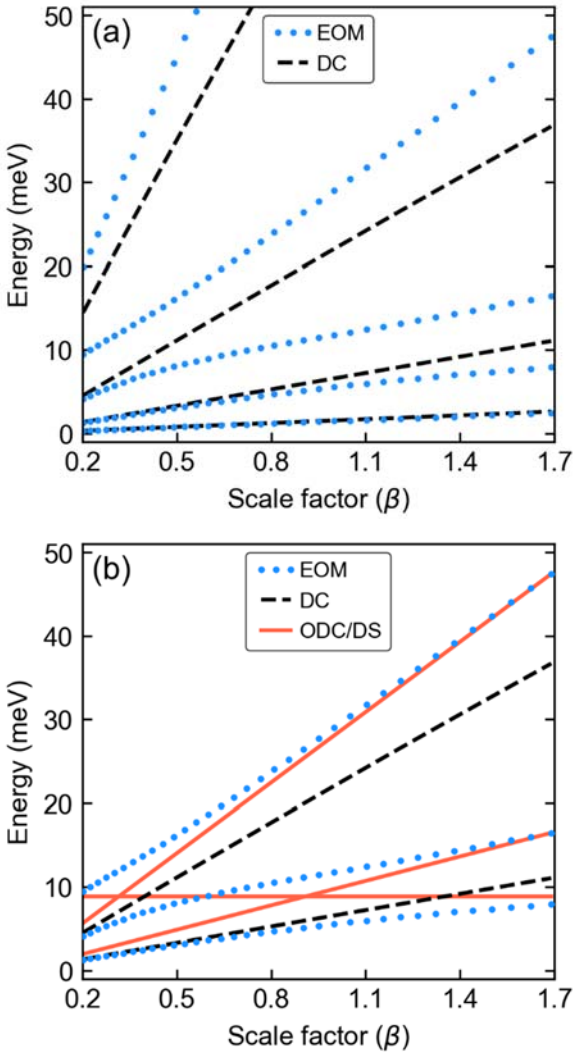

Figure 2. (a) Stabilization graph for $(NaCl)_2$ obtained from EA-EOM-CCSD calculations at $q = 0$ and using the correlated core approximation. The energies of the excess electron states from EOM-CCSD calculations and of the DC levels are shown as blue dots and black dashed lines, respectively. (b) The energies of the excess electron states from EOM-CCSD calculations are shown as blue dots. The energies of the DC levels are shown as black dashed lines and the unmixed discrete level by the horizontal red line, while estimates of the energies of the second and third DC levels orthogonalized to the discrete level is indicated by the sloped red line.

where H_{11} is the energy if the discrete state, H_{22} is the energy of the appropriate DC level, V is the coupling between the discrete state and the DC level, and S is the overlap of the associated wave functions. At β = 1.3, where the discrete level and the second DC level cross, one can use the energies of the diabatic and adiabatic levels to determine that $S = 0.52$ and $V = 1.86$ meV (at that β value).

Figure 3 plots, as a function of q, the energy for the B_{2u} anion state obtained from EA-EOM-CCSD calculations carried out both with the FC and correlated core approximations. (A value of $q = 0.1$ corresponds to an increase of the Na-Na distance by 0.118 Å and an increase in the Cl-Cl distance by 0.078 Å). For q values at which the anion is unbound, the results were obtained using the stabilization procedure described above, and we plot both E_r and Γ/2. In both sets of calculations the real part of the energy of the TA is seen to be a smooth continuation of the energy of the bound state, as q is decreased. The inclusion of correlation effects involving the Na core electrons increases the attraction of the electron for the cluster: the stabilization is ~9 meV at $q = 0.15$, at which the anion is bound, and ~3.5 meV at $q = 0$ at which the

B_{2u} anion is unbound. (The smaller stabilization at $q = 0$ is consistent with the more extended charge distribution of the anion when it is temporary than when it is bound.) As a result, both E_r and Γ are predicted to be smaller in the calculations correlating the core electrons of the Na atoms than in those carried out using the FC approximation at a given value of q. The resonance energy was also calculated at the geometry of the neutral cluster optimized at the MP2 level in the correlated core approximation, with the resulting values of E_r and Γ/2 being 14.40 and 8.94 meV, respectively. It should be noted that the geometry optimized at this level of theory is very close to that obtained in the FC approximation with q displaced to -0.05233, at which stabilization calculations making use of the correlated core approximation give values of E_r and Γ/2 (13.67 and 8.05 meV, respectively) that are within 1 meV of the resonance parameters obtained using the geometry optimized in the correlated core approximation.

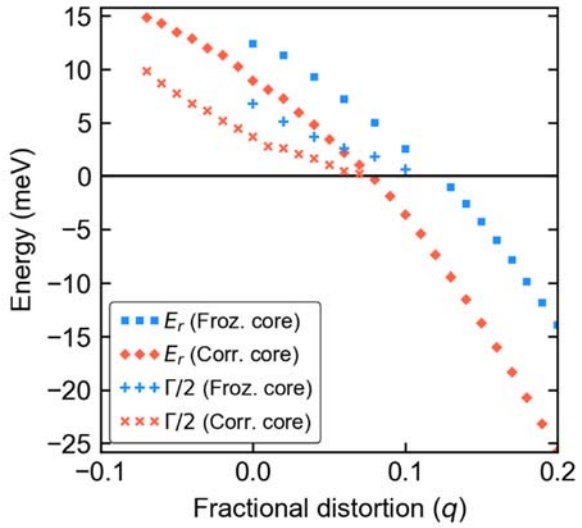

Figure 3. Resonance energy, E_r and Γ/2, from EA-EOM-CCSD stabilization calculations on the B_{2u} anion of $(NaCl)_2$ as a function of q, the distortion along the symmetric breathing normal coordinate. Results obtained in the frozen core (shown in blue) and correlated core (shown in red) approximations are reported. The figure also includes the negative of the EBE for q values for which the anion is bound.

While the use of the correlated core approximation impacts both E_r and Γ, when Γ/2 is plotted vs E_r for the q values for which the anion is predicted to be temporary, the results from the stabilization calculations with and without correlation of the Na core electrons, are found to essentially fall on the

same curve as seen in Figure 4. This is consistent with the fact, discussed in detail later, that correlating the Na core electrons impacts the electron-cluster interaction potential only at short-range and has negligible impact on the barrier region which controls the width (for a given value of E_r).

Also shown in Figure 4 are least squares fits of Γ/2 as a function of E_r for the core-correlated calculations using threshold laws[39] assuming either *p*-wave (dashed black line) or *f*-wave (red dotted line) character of the resonance. (Symmetry constrains the resonance to contain only odd ℓ angular momentum terms.) The equations used in the fits are:

$$\frac{\Gamma}{2}(\ell = 1) = \frac{AE_r^{3/2}}{1+BE_r} \quad (5a)$$

$$\frac{\Gamma}{2}(\ell = 3) = \frac{AE_r^{3.5}}{225+45(BE_r)+6(BE_r)^2+(BE_r)^3} \quad (5a)$$

The fit based on eq 5a (with A = 0.172 and B = 0.037) is superior to that obtained assuming purely *f*-wave character (with A = 15.97 and B = 2.14). We note that, while the fit was based only on the data from the core-correlated calculations with q ranging from 0.07 to 0 (E_r ranging from approximately 1 – 9 meV), the best-fit curve was extended over the entire range of q values considered. The departure of the fit from the data from the smaller q values suggests that for these points the threshold formula is beginning to fail. At q = 0 in the correlated core approximation the width, Γ is already about 80% as large as E_r, and the resonance cannot be considered narrow.

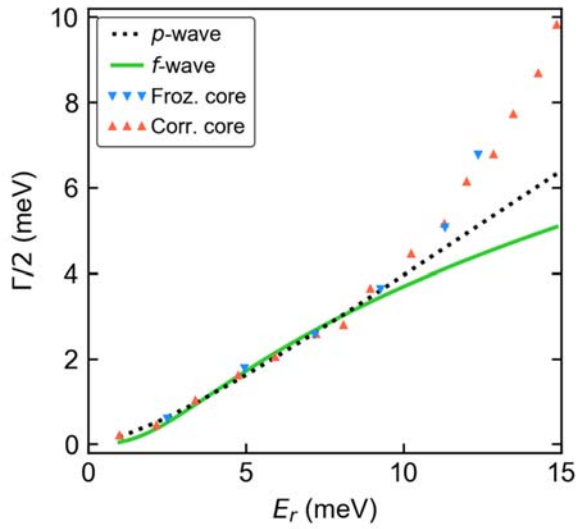

Figure 4. Γ/2 vs E_r from EA-EOM-CCSD/stabilization calculations on the B_{2u} anion of $(NaCl)_2$ with the results from the frozen core and correlated core approximations shown as blue triangles and red triangles, respectively. Also shown are fits based on eq 5, with the fit using the expression for a *p*-wave resonance shown as the black dotted line and that for an *f*-wave resonance shown as the solid green line.

III.2 Polarization and effective potentials for e^- + $(NaCl)_2$. In light of the finding that inclusion of correlation effects involving the core electrons of the Na atoms impacts the energies of the anion states, we find it instructive to examine the polarization potential of $(NaCl)_2$ calculated in the FC and correlated core approximations. Figure 5 plots, along the NaNa axis, the polarization potential of $(NaCl)_2$ calculated at the MP2 level in both the FC and correlated core approximations. As seen from this figure, the polarization potential is much more attractive in the correlated core approximation. These results were obtained by subtracting the MP2-level electrostatic potential from the change in the MP2 energy caused by a negative point charge at various locations along the NaNa axis. It should be noted that similar results are obtained in the HF approximation which means that the increased attraction of the polarization potential close to the Na atoms is predominantly due to the inclusion of basis functions appropriate for describing polarization of the core electrons rather than to correlation of the core. However, it is important to note that in the calculation of the EBE's of the anions, this is manifested in terms of correlation effects involving the diffuse excess electron and the tightly bound electrons of the Na cores.[40] Although both the

A_g and the B_{2u} anions have very extended charge distributions, the small amount of charge density of the excess electron near the Na cores results in a non-negligible stabilization of the anion when correlation effects between the excess electron and the core electrons is included.

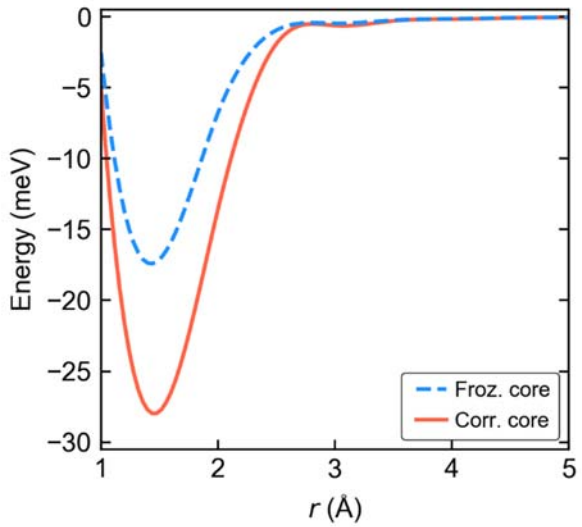

Figure 5. The polarization potential for the correlated core (solid red line) and frozen core (dashed blue line) as a function of distance along the Na-Na axis (r, in Angstroms).

As noted in the Introduction, shape resonances can be viewed as resulting from the trapping of an excess electron in the effective potential describing the electron-molecule interaction. In light of this, it is instructive to consider the effective potential for a purely p-wave resonance of $(NaCl)_2$. Figure 6 plots the polarization, electrostatic, and angular momentum contributions to the effective potential obtained in the correlated core approximation at $q = 0$. The polarization and electrostatic contributions to the effective potential were obtained by applying the procedure of Boardman et al.[41] to the results of MP2 calculations of the electrostatic potential and of the energy of the cluster interacting with a negative point charge at various locations. The most striking aspect of the net effective potential is the large distance of the barrier from the center of the molecule: The maximum of the barrier occurs near an electron-molecule distance of 14 Å at which the energy is 13.2 meV, about 4 meV above the value of E_r calculated for the B_{2u} resonance at $q = 0$. Polarization effects are negligible in the barrier region, and the barrier results from the interplay of the attractive electrostatic interaction and the repulsive angular momentum term. The distance

of the barrier from the molecule is much greater than found for valence shape resonances for which the barrier results from the interplay of the polarization and angular momentum contributions. We note that the effective potential shown in Figure 6 does not account for exchange between the excess electron and the electrons of the cluster or for orthogonality of the orbital occupied by the excess electron to the orbitals of the cluster of the same symmetry. Both of these effects are short-ranged and are not expected to impact the barrier region of the potential.

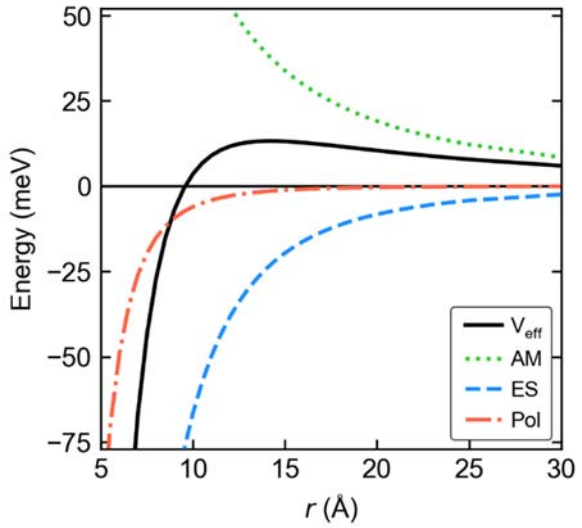

Figure 6. Effective radial potential, V_{eff} (solid black line), vs r, the distance from the center of the cluster, for p-wave scattering from the $(NaCl)_2$ cluster model with $q = 0$. The electrostatic contribution (ES) is shown as the dashed blue line, the polarization contribution (Pol) is shown as the red dash-dotted line, and the angular momentum contribution (AM) is shown as the green dotted line.

III.3. Potential energy curves. Figure 7 reports as a function of q the potential energy curves for the ground state of the neutral cluster as well as for the A_g and B_{2u} anion states. The total energy of the neutral molecule is from CCSD calculations, and the energies of the anion states are obtained by subtracting the EBEs from the EOM-CCSD calculations from the energies of the neutral. These curves were generated allowing for core correlation. For q-values at which the B_{2u} state lies higher in energy than the neutral cluster, the EBEs are associated with the negative of the real parts of the resonance energy from the stabilization calculations. The energies of both anion states display a q-dependence similar to

that of the neutral, consistent with the extra electron occupying a highly extended non-valence orbital. Whereas the A_g state is bound by approximately 150 meV over the entire range of q values considered, the energy of the B_{2u} state is very close to that of the neutral, being bound only for $q \gtrapprox 0.08$.

Based on the potential energy curves depicted in Figure 7, the B_{2u} anion of rhombic $(NaCl)_2$ should be detectable by IR absorption from the bound A_g anion state. However, it should be noted that Anusiewicz et al. found in their computational study that the ground state anion distorts from the rhombic to a C_{2v} structure. The energy lowering associated with this distortion was so small that these authors concluded that the structure averaged over the vibrational zero-point motion would still be D_{2h}. This distortion is presumably driven by the enhanced electron binding due to the accompanying dipole moment (~1.5 D in the calculations of Anusiewicz et al.). At the distorted structures the excited state anion would acquire *s*-wave character which would act so as to shorten the anion lifetime, and which could make its detection in IR absorption from the ground state anion more challenging.

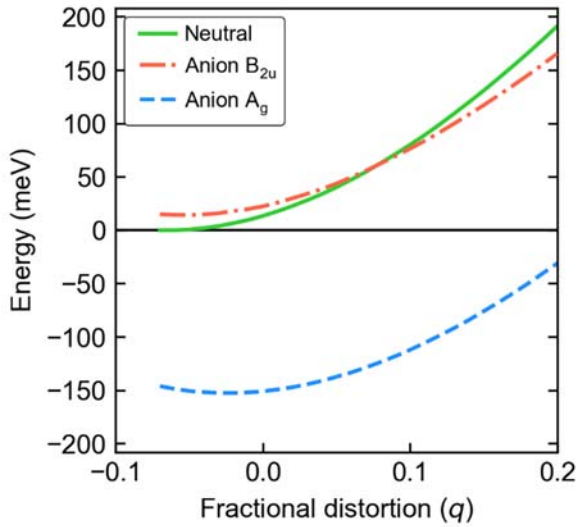

Figure 7. Relative energies of the A_g (dashed blue) and B_{2u} (dash-dotted red) anion states and of the ground state of the neutral $(NaCl)_2$ cluster (solid green) as a function of q, the fractional distortion along the symmetric breathing normal coordinate. The energy of the neutral ground state at its most stable geometry (q = -0.06) is taken as the zero of the energy scale. The energy of the neutral is from CCSD calculations and the energies of the anion states are from the EOM-CCSD calculations, all obtained using the correlated core approximation.

Table 1 reports the EBE obtained using various theoretical methods of the A_g anion at $q = 0$. For the A_g state the FC and correlated-core EBEs obtained using the EA-EOM-CCSD method are 139 and 164 meV, respectively. Thus, core correlation is more important for the A_g anion than for the B_{2u} temporary anion, consistent with the more diffuse charge distribution of the latter. Table 1 also includes EBEs calculated using the EOM-CCSD(T)(a)* method as well as with the ΔCCSD and ΔCCSD(T) methods. (The Δ methods involve calculating separately the energies of the ground neutral and the anion, and are feasible only for anion states that demonstrate binding in the HF approximation.) The EOM-CCSD(T)(a)* and ΔCCSD(T) methods give EBEs that agree to within 1 meV of each other, with the EOM-CCSD(T)(a)* results being 148 and 176 meV in the FC and correlated core approximations, respectively. This shows that correlation of the Na core electrons is ~4 meV more important in the EOM-CCSD(T)(a)* than in the EA-EOM-CCSD calculations, and also that inclusion of higher order correlation effects absent in the EA-EOM-CCSD method lead to a 12 meV increase in the EBE of the A_g anion.

Table 1. Electron Binding Energy (meV) of the A_g anion state of $(NaCl)_2$ calculated at various levels of theory in the frozen core and correlated core approximations

core	EOM-CCSD	EOM-CCSD(T)a*	ΔCCSD	ΔCCSD(T)
Frozen	139	148	128	147
Correlated	164	176	152	175

At $q = 0$, the EA-EOM-CCSD calculations predict the B_{2u} anion state to be unbound with respect to the neutral by 12.4 and 9.0 meV in the FC and correlated-core approximations, respectively. As we saw above, higher order correlation effects (not included in EOM-CCSD) stabilize the A_g anion state by about 12 meV, making it important to estimate their effect on the B_{2u} anion at q values that the EOM-CCSD calculations predict it to be a resonance. To this end we also carried out EOM-CCSD(T)(a)* calculations to the B_{2u} anion at q values at which the anion is bound. We did such calculations at $q = 0.20$ and 0.15, and find that the use of EOM-CCSD(T)(a)* rather than EA-EOM-CCSD increases the EBEs at these q

values by only 3.0 and 2.5 meV, respectively. Higher order correlation effects are expected to be even less important at q values at which the anion is metastable. Indeed, stabilization calculations carried out using the EOM-CCSD(T)(a)* method at the geometry of the neutral cluster optimized at the MP2 level in the correlated core approximation showed that the resonance energy and width are impacted by less than 1 meV by the inclusion of higher order correlation effects.

IV. CONCLUSIONS

In this study, we present the results of calculations that indicate that $(NaCl)_2$, at its equilibrium geometry, possesses both a bound non-valence anion of A_g symmetry and a non-valence temporary anion of B_{2u} symmetry. Inclusion of correlation of the Na core electrons is found to significantly impact the geometry of $(NaCl)_2$ and the energies of the A_g and B_{2u} anion states, although this is less important for the B_{2u} anion at geometries at which the anion is a resonance than those at which it is bound. Electron correlation effects recovered by the EOM-CCSD(T)(a)* method but lacking in EOM-CCSD are found to lead to a ~12 meV increase of the EBE of the A_g anion (at $q = 0$), but have a smaller impact on the EBE of the B_{2u} anion. The B_{2u} temporary anion state of $(NaCl)_2$ in its rhombic structure should manifest itself both in low-energy electron scattering from neutral cluster as well as in the IR photodetachment of the excess electron from the bound A_g anion. In the latter case, the resonant and direct detachment channels are expected to interfere, thereby modifying the Fano lineshape.[42]

Acknowledgments: KDJ and AK acknowledge support from the National Science Foundation under grant CHE1762337. We also acknowledge the use of computational resources provided by the University of Pittsburgh's Center for Research Computing.

References:

1. Koopmans, T. Über die Zuordnung von Wellenfunctionen und Eigenwerten zu den Einzelnen Elektronen Eines Atoms. *J. Phys. B* **1934**, *1*, 104-113.

2. Simons J.; Jordan, K. D. *Ab Initio* Electronic Structure of Anions. *Chem. Rev*. **1987**, *87*, 535-554.

3. Wang F.; Jordan, K. D. Theory of Dipole-Bound Anions. *Annu. Rev. Phys. Chem*. **2003**, *54*, 367-396.

4. Desfrançois, C.; Abdoul-Carime, H.; Schermann, J.-P. Ground-State Dipole-Bound Anions. *Int. J. Mod. Phys. B* **1996**, *10*, 1339-1395.

5. Sommerfeld, T. Multipole-Bound States of Succinonitrile and other Dicarbonitriles. *J. Chem. Phys*. **2004**, *121*, 4097-4104.

6. Desfrançois, C.; Bouteiller, Y.; Schermann, J. P.; Radisic, D.; Stokes, S. T.; Bowen, K. H.; Hammer, N. I.; Compton R. N. Long-Range Electron Binding to Quadrupolar Molecules. *Phys. Rev. Lett.* **2004**, *92*, 083003.

7. Bezchastnov, V. G.; Vysotskiy, V. P.; Cederbaum, L. S. Anions of Xenon Clusters Bound by Long-range Electron Correlations. *Phys. Rev. Lett.* **2011***, 107*, 133401.

8. Voora, V.; Cederbaum, L. S.; Jordan, K. D. Existence of a Correlation Bound *s*-type Anion State of C_{60}. *J. Phys. Chem. Lett*. **2013**, *4*, 849-853.

9. Voora, V. K.; Jordan, K. D. Non-valence Correlation-Bound Anion State of C_6F_6: Doorway to Low-Energy Electron Capture. *J. Phys. Chem. A*. **2014**, *118*, 7201-7205.

10. Voora, V. K.; Kairalapova, A.; Sommerfeld, T.; Jordan, K. D. Theoretical Approaches for Treating Non-Valence Correlation-Bound Anions. *J. Chem. Phys*. **2017**, *147*, 214114:1-11.

11. Schulz, G. J. Resonances in Electron Impact on Diatomic Molecules. *Rev. Mod. Phys*. **1973**, *45*, 423-486.

12. Jordan, K. D.; Burrow, P. D. Temporary Anion States of Polyatomic Hydrocarbons". *Chem.*

Rev., **1987**, *87*, 557-588.

13. Jordan, K. D.; Burrow, P. D. Studies of the Temporary Anion States of Unsaturated Hydrocarbons by Electron Transmission Spectroscopy. *Acc. Chem. Res*. **1978**, *11*, 341-348.

14. Stanton, J. F.; Gauss, J. Perturbative Treatment of the Similarity Transformed Hamiltonian in Equation-of-Motion Coupled-Cluster Approximations. *J. Chem. Phys*. **1995**, *103*, 1064-1076.

15. Kairalapova, A.; Jordan, K. D.; Maienshein, D. N.; Fair, M. C.; Falcetta, M. F. Prediction of a Non-Valence Temporary Anion Shape Resonance for a Model $(H_2O)_4$ System. *J. Phys. Chem. A* **2019**, *123*, 2719–2726.

16. Jagau, T.-C.; Dao, D. B.; Holtgrewe, N. S.; Krylov, A. I.; Mabbs, R. Same but Different: Dipole-Stabilized Resonances in CuF^- and AgF^-. *J. Phys. Chem. Lett.* **2015**, *6*, 2786-2793.

17. Skomorowski, W.; Gulania, S.; Krylov, A. I. Bound and Continuum-Embedded States of Cyanopolyyne. *Phys. Chem. Chem. Phys.* **2018**, *20*, 4805-4817.

18. Oana, C. M.; Krylov, A. I. Dyson Orbitals for Ionization from the Ground and Electronically Excited States within Equation-of-Motion Coupled-Cluster Formalism: Theory, Implementation, and Examples. *J. Chem. Phys.* **2007**, *127*, 234106.

19. Anusiewicz, I.; Skurski, P.; Simons, J. First Evidence of Rhombic $(NaCl)_2^-$. Ab Initio Reexamination of the Sodium Chloride Dimer Anion. *Phys. Chem. A* **2002**, *106*, 4410636-10644.

20. Sommerfeld, T.; Bhattarai, B.; Vysotskiy, V. P.; Cederbaum, L. S. Correlation-bound Anions of NaCl Clusters. *J. Chem. Phys.* **2010**, *133*, 114301

21. Raghavachari, K.; Trucks, G. W.; Pople, J. A.; Head-Gordon, M. A. Fifth-order Perturbation Comparison of Electron Correlation Theories. *Chem. Phys. Lett.* **1989**, *157*, 479.

22. Hotop, H.; Ruf, M.-W.; Allan, M.; Fabrikant I. I. Resonance and Threshold Phenomena in Low-Energy Electron Collisions with Molecules and Clusters. *Adv. At. Mol. Opt. Phys*. **2003**, *49*, 85-216.

23. Møller, C.; Plesset, M. S. Note on an Approximation Treatment for Many-Electron Systems. *Phys. Rev*. **1934**, *46*, 618-622.

24. Kendall, R. A.; Dunning, Jr., T. H.; Harrison, R. J. Electron Affinities of the First-Row Atoms Revisited. Systematic Basis Sets and Wave Functions. *J. Chem. Phys*. **1992**, *96*, 6796-6806.

25. Dunning, Jr., T. H. Gaussian Basis Sets for Use in Correlated Molecular Calculations. I. The Atoms Boron through Neon and Hydrogen. *J. Chem. Phys*. **1989**, *90*, 1007-1023.

26. Falcetta, M. F.; DiFalco, L. A.; Ackerman, D. S.; Barlow, J. C.; Jordan, K. D. Assessment of Various Electronic Structure Methods for Characterizing Temporary Anion States: Application to the Ground State Anions of N_2, C_2H_2, C_2H_4 and C_6H_6. *J. Phys. Chem. A* **2014**, *118*, 7489-7497.

27. Jagau, T.-C.; Zuev, D.; Bravaya, K. B.; Epifanovsky, E.; Krylov, A.I. A Fresh Look at Resonances and Complex Absorbing Potentials: Density Matrix-Based Approach. *J. Phys. Chem. Lett*. **2014**, *5*, 310-315.

28. Bhaskaran-Nair, K.; Kowalski, K.; Jarrell, M.; Moreno, J.; Shelton, W. A. Equation of Motion Coupled Cluster Methods for Electron Attachment and Ionization Potential in Polyacenes. *Chem. Phys. Lett.* **2015**, *641*, 146-152.

29. Matthews, D. A.; Stanton, J. F. A New Approach to Approximate Equation-of-Motion Coupled Cluster with Triple Excitations *J. Chem. Phys.* **2016**, *145*, 124102.

30. Prascher, B. P.; Woon, D. E.; Peterson, K. A.; Dunning, Jr., T. H.; Wilson, A. K.; Gaussian Basis Sets for use in Correlated Molecular Calculations. VII. Valence and Core-valence Basis Sets for Li, Na, Be, and Mg. *Theor. Chem. Acc.* **2011**, *128*, 69.

31. CFOUR Stanton, J. F.; Gauss, J.; Harding, M.; Szalay, P. CFOUR, Coupled-Cluster Techniques for Computational Chemistry (2010).

32. Siegert, A. J. On the Derivation of the Dispersion Formula for Nuclear Reactions. *Phys. Rev*. **1939**, *56*, 750-752.

33. Hazi, A. U.; Taylor, H. S. Stabilization Method of Calculating Resonance Energies: Model Problem. *Phys. Rev A* **1970**, *1*, 1109-1120.

34. Chao, J. S.-Y.; Falcetta, M. F.; Jordan K. D. Application of the Stabilization Method to $N_2^-(1^2\Pi_g)$ and $Mg^-(1^2P)$ Temporary Anion States. *J. Chem. Phys*. **1990**, *93*, 1125-1135.

35. McCurdy, C. W.; McNutt, J. F. On the Possibility of Analytically Continuing Stabilization Graphs to Determine Resonance Positions and Widths Accurately. *Chem. Phys. Lett*. **1983**, *94*, 306-310.

36. Isaacson A. D.; Truhlar, D. G. Single-root, Real-basis-function Method with Correct Branch-point Structure for Complex Resonances Energies. *Chem. Phys. Lett.* **1984**, *110*, 130-134.

37. Jordan, K. D.; Voora, V. K.; Simons, J. Negative Electron Affinities from Conventional Electronic Structure Methods, *Theor. Chem. Acc.*, **2014**, *133*, 1445:1-15.

38. Gaussian 16, Revision B.01, Frisch, M. J.; Trucks, G. W.; Schlegel, H. B.; Scuseria, G. E.; Robb, M. A.; Cheeseman, J. R.; Scalmani, G.; Barone, V.; Petersson, G. A.; Nakatsuji, H.; et al. Gaussian, Inc., Wallingford CT, 2016.

39. Blatt, J.; Weiskopf, V. F. *Theoretical Nuclear Physics*, publ. Wiley (1952).

40. Sommerfeld, T.; DeFusco, A.; Jordan, K. D. Model Potential Approaches for Describing the Interactions of Excess Electrons with Water Clusters: Incorporation of Long-range Correlation Effects. *J. Phys. Chem. A* **2008**, *112,* 11021-11035.

41. Boardman, A. D.; Hill, A. D.; Sampanthar, S. Partial Wave Scattering by Non-Spherically Symmetric Potentials. I. General Theory of Elastic Scattering. *Phys. Rev*. **1967**, *160*, 472-475.

42. Fano, U. Effects of Configuration Interaction on Intensities and Phase Shifts. *Phys. Rev.* **1961**, *124,* 1866–1878.

TOC Graphic

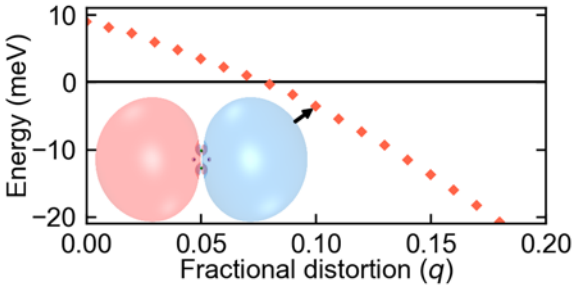
10
0
−10
−20
Energy (meV)
0.00
0.05
0.10
0.15
0.20
Fractional distortion (q)